Photo-Induced Dissociation of Protonated Peptide Ions in a Quadrupole Ion Trap Time-of-Flight Mass Spectrometer

Tae Oh Yoon, Chang Min Choi, Hwan Jin Kim, and Nam Joon Kim*

*Department of Chemistry, Chungbuk National University, Chungbuk 361-763, Korea. *E-mail: namjkim@chungbuk.ac.kr*

We have constructed a quadrupole ion trap time-of-flight mass spectrometer to study photo-induced dissociation (PID) of biologically important molecules in the gas phase. The performance and capabilities of the mass spectrometer were investigated by measuring the mass spectra of protonated peptide ions produced by electrospray ionization. The typical mass resolution ($m/\Delta m$) was around 1000 and the collection efficiency measured for photo-fragment ions of protonated Tyr-Ala ions (YAH^-) was about 41%. The PID spectra of YAH^- and protonated Gly-Trp ions (GWH^+) were compared to their respective spectra obtained by collision-induced dissociation in the same instrument. The chromophore effect in photodissociation of protonated peptide ions was addressed with the PID spectrum of GWH^-.

Key Words : Quadrupole ion trap, Time-of-flight mass spectrometer, Photo-induced dissociation, Protonated peptide ion

Introduction

The combination of a quadrupole ion trap (QIT) with a time-of-flight mass spectrometer (TOFMS) provides a powerful tool to study photo-induced dissociation (PID) as well as collision-induced dissociation (CID) dynamics of large biomolecules such as peptides and proteins produced by electrospray ionization (ESI).[1-3] It incorporates some of the best features of each instrument. TOFMS can measure a whole mass spectrum in a few tens of μsec, which enables the detection of intermediate species generated in an ion-molecule reaction. In addition, it can detect ions in the theoretically unlimited mass range with high transmission. TOFMS is also simple and robust so that it can be easily built in the laboratory. The main disadvantage, however, is that TOFMS intrinsically operates in a pulse-mode. Therefore, when it combines with a continuous ionization source, the loss of sensitivity is inevitable due to the low duty cycle of a TOFMS.

The quadrupole ion trap is also a powerful mass analyzer with many distinct advantages.[4,5] It can store ions of wide mass ranges for an extended period of time. It was recently reported that the masses of single bacterial whole cells ($\sim10^{10}$ dalton) could be measured with a quadrupole ion trap.[6] In addition, the ion trap can perform multiple stages of tandem in time mass spectrometry for structural analysis of the samples. The disadvantage, however, is that we have to scan the amplitude or the frequency of the radio frequency (rf) signal applied to the ion trap for mass analysis. Since the mass resolution is inversely proportional to the scanning rate, it typically takes from seconds to a few tens of minutes to get an entire mass spectrum with a pertinent resolution.

To make the best of advantages of both a TOFMS and a QIT, and to offset their disadvantages all together, Lubman and coworkers[7] first developed a quadrupole ion trap time-of-flight mass spectrometer (QIT-TOFMS). In this mass spectrometer. QIT interfaces a continuous ESI source with a TOFMS in a pulse-mode. The QIT stores ions produced continuously by an ESI source for a certain period of time and then pulses them out into the TOFMS for mass analysis by applying dc pulses to the endcaps of the QIT. As a result, nearly 100% duty cycle of a TOFMS is achieved even with a continuous ionization source like the ESI.

Many studies have been performed using this type of a hybrid mass spectrometer. The PID of peptide ions has been studied by irradiating IR^{2-8} or UV beams onto the ions in the trap.[9] The photodissociation dynamics of multiply charged ions, ligated/solvated transition metal dications and metal cluster ions were investigated using optical spectroscopy.[10,11] The dissociation dynamics of single amino acid or peptide ions[12] were studied using nanosecond and femtosecond laser pulses.[13] The quantitative capabilities of a QIT-TOFMS were investigated by analyzing pharmaceutical or environmental compounds.[14] Combined with high performance liquid chromatography, QIT-TOFMS was also used to identify proteins from 2D gel electrophoresis of human erythroleukemia cells.[15] Even the photoelectron spectroscopy of multiply charged anions has been performed using the QIT-TOFMS combined with a TOF photoelectron spectrometer.[16]

Some modifications have also been followed to improve the performance of a QIT-TOFMS. Instead of an ESI source, the matrix assisted laser desorption/ionization (MALDI) source was employed.[17] A new hybrid mass spectrometer combining a QIT with an orthogonal TOFMS was constructed.[18] Douglas and coworkers[19] even uses a linear ion trap, instead of a QIT, with an orthogonal TOFMS to increase the capacity of ion storage.

In this paper, we report the construction of a QIT-TOFMS, which has basically the same structure with that developed by Lubman and coworkers.[7] to study photodissociation dynamics of protonated peptide or protein ions produced by ESI. Some modifications by us were the extra holes drilled

on the QIT for collecting laser-induced fluorescence from ions inside the trap (not used in this study). The performance and capabilities of the newly-built QIT-TOFMS were investigated by measuring a mass spectrum of melittin ions and also the PID or CID spectra of protonated Tyr-Ala (YAH⁻) and Gly-Trp (GWH⁻) ions.

Experimental

The schematic diagram of the experimental apparatus is shown in Figure 1. It consists of three differentially pumped chambers: the source, the main and the detection chamber. The source chamber was evacuated by a mechanical pump (600 L/min) and, the main and the detection chamber were pumped by a 6" and a 4" diffusion pump (DP), respectively. To prevent oil backstreaming, a liquid nitrogen trap was placed on top of the 6" DP. Both DPs were filled with Santovac 5 as the pumping fluid to reduce background ion signals from the oil adducts produced inside the ion trap.[20] The operating pressures of the source, the main and the detection chamber were 5.2×10^{-1}, 3.4×10^{-4} and 1.6×10^{-6} Torr, respectively.

A. Electrospray ionization source. Melittin, Tyr-Ala and Gly-Trp were purchased from Sigma and used without further purification. The powder sample was dissolved in the solvent mixture of methanol, water and acetic acid (48.5: 48.5:3 by volume) at a concentration of 100 μM.

The syringe pump (KD scientific, Model 100) transferred the peptide solution to the source chamber through a fused silica capillary. The flow rate was maintained to be 400 μL/ h. The fused sillica capillary was connected to an electrospray nozzle with an orifice of 76 μm in diameter (dia.) inside a zero-dead-volume tee (Upchurch scientific, P-775) where a platinium wire, which was floated to +3.5 kV, was also inserted perpendicularly to both the capillary and the nozzle.

The ion spray from the nozzle entered into a heated capillary tube (20-cm long, 1/16" OD, 0.75-mm ID) that was tightly fitted into a 1/8" copper tube. The outside of the copper tube was wound with a heating tape for heating up to 200 °C. The ions were desolvated while passing through the heated capillary and then entered into the main chamber through a skimmer with a hole of 0.38-mm dia.

B. Trapping and TOF operation. The ions through the skimmer were spatially focused by an einzel lens into a 3-

mm hole of the entrance endcap of a QIT (R.M. Jordan Co.). The QIT consists of one ring and two endcap electrodes. Each endcap has a hole of 3-mm dia. for ion beams to enter and exit. There are also four holes of 2.2-mm dia. in the ring electrode. Two holes are for laser beams to enter and exit, and the others for detection of laser-induced fluorescence from ions inside the ion trap. An extra inlet tube is connected into the ceramic space of the ion trap for addition of a collision gas.

To store ions in the QIT, the rf signal of a constant frequency (1 MHz) and amplitude (+2 kV) was applied to the ring electrode while both endcaps were grounded. By altering the rf amplitude, we could vary the m/z range of ions stored in the QIT. After a certain time of ion storage, a positive and a negative dc pulse were applied simultaneously to the entrance and the exit endcap, respectively, to extract all of the ions inside the QIT into the TOFMS. During this extraction, the rf voltage was turned off to reduce any deteriorating effects of the rf field on ion trajectories.

The extracted ions were accelerated toward a field-free region of a reflectron TOFMS (R.M. Jordan Co.) where the flight tube was floated to −1.5 kV for further acceleration of the ions. Then, the ions were detected by a 40-mm dual microchannel plate (MCP). The face of the first plate was floated to −2.2 kV. The ion signals from the MCP were processed by a 400 MHz digital storage oscilloscope (LeCroy, 9310A).

The timings of the trapping, the extraction and the detection were synchronized by TTL pulses from a digital delay generator (SRS, DG 535).

C. Laser system. For PID experiments, the frequency-doubled output (1-2 mJ/pulse) of a dye laser (Scanmate 2) pumped by the second harmonic of an Nd:YAG laser (Surelite II) was focused by a lens of 25-cm focal length and then irradiated onto the ions in the QIT right before the extraction dc pulses were applied. Light baffles were placed inside of the entrance and the exit port of the light to reduce any possible electrical noises generated by the scattered light.

Results and Discussion

To know the performance and characteristics of the newly-built QIT-TOFMS and also its capability for studies on PID of protonated peptide ions, we obtained the mass spectrum
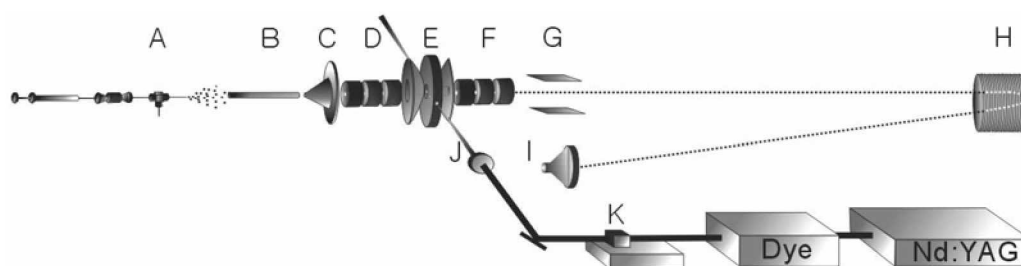

Figure 1. Schematic diagram of the experimental apparatus. (A) ESI source, (B) heated capillary, (C) skimmer, (D) the 1st einzel lens, (E) QIT, (F) the 2nd einzel lens, (G) deflector, (H) reflectron, (I) MCP, (J) optical lens, (K) BBO crystal.
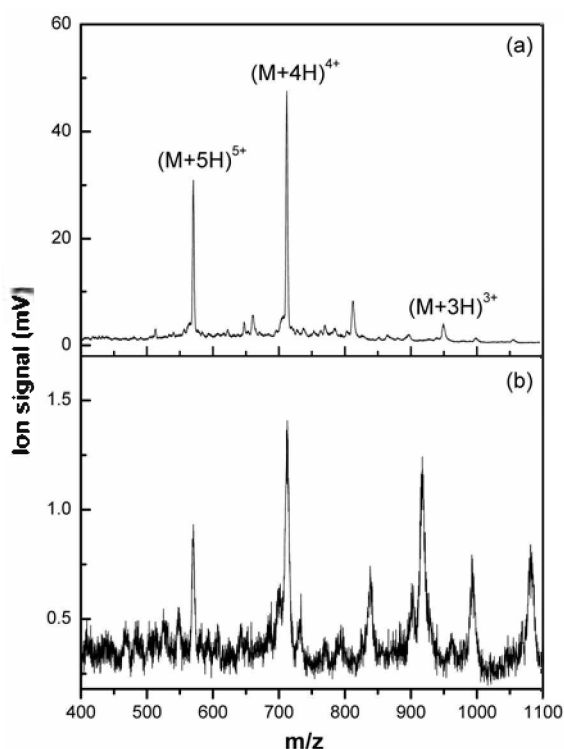
Figure 2. Mass spectra of melittin ions produced by ESI (a) with and (b) without helium gas in the ion trap. The pressure of the main chamer increased to 5×10^{-4} torr with the helium gas.

Figure 3. (a) Mass spectrum of YAH^+ with helium gas in the ion trap. The inset is an enlarged view of the YAH^+ peak at m/z 253. (b) PID spectrum obtained by irradiating laser pulses (2 mJ/pulse) at 277 nm onto the ions in the QIT. (c) Difference spectrum obtained by subtracting the laser-off signals from the laser-on. (d) CID spectrum obtained by introducing argon into the QIT as a collision gas. The pressure of the main chamer increased to 7×10^{-4} torr with the argon gas. The inset is an enlarged view of the fragments of m/z 136 and 137 that were detected at the lower argon pressure of the ion trap.

of melittin (MW 2846.46) ions as well as those of YAH^+ and GWH^- using a PID or a CID method

Figure 2 shows the mass spectra of melittin ions produced by ESI. The multiply charged ions, which are a characteristic of ESI, are clearly seen from $(M+5H)^{5+}$ to $(M+3H)^{3+}$. The ion signal of $(M+4H)^{4+}$ is the strongest and that of $(M+3H)^{3+}$ is the weakest. Although the relative intensities among multiply charged ions varied with the rf voltage applied to the ion trap, the $(M+4H)^{4+}$ remained to be the strongest with rf voltages of +1.9~3 kV. This agrees well with the previous report.[7]

The interesting observation in Figure 2 was that addition of helium gas to the ion trap significantly improved both the sensitivity and the mass resolution of the QIT-TOFMS. With helium gas in the ion trap, the ion intensity of $(M+4H)^{4+}$ increased by 30 times and the mass resolution became three-fold higher than those measured without the helium gas. This goes in parallel with the previous observation.[14] They suggested that the cooling of ions through the multiple collisions with the helium gas was responsible for these improvements.

Figure 3a is the mass spectrum of YAH^+ (m/z 253). Only the singly charged ions of YAH^- were observed in the mass spectrum with little fragment ions of them. The mass resolution was calculated to be around 1000 using the full width at half maximum (FWHM) of the YAH^- peak. This resolution is as high as that of the first QIT-TOFMS constructed by Lubman and coworkers.[7]

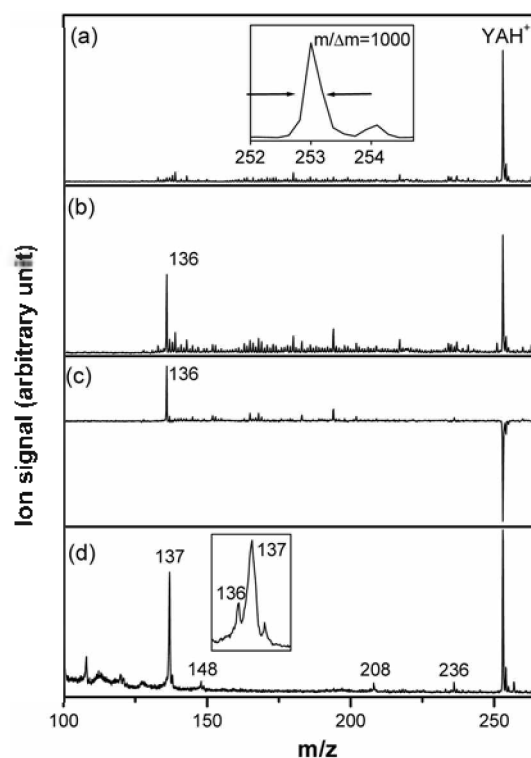Figure 3b is the mass spectrum measured following irradi-

ation of laser pulses at 277 nm into the ion trap. The wavelength was chosen because YH^- has broad electronic absorption around this wavelength.[21] The difference spectrum in Figure 3c was obtained by subtracting the laser-off signals from the laser-on. Thus, the negative signal at m/z 253 in the spectrum represents the depleted ion intensity and the positive signal at m/z 136 represents fragment ions produced by PID of YAH^+. No other photo-fragment ions were detected, even with the lower rf voltages down to +1.5 kV with which much smaller ions could be trapped inside the ion trap. Therefore, by measuring intensities of the photo-fragment and the depleted parent ions, we could calculate the lower limit of the collection efficiency for photo-fragment ions. It was around 41% with the trapping time of 500 msec and the rf voltage of +2 kV. The PID efficiency of YAH^+ at this wavelength (~2 mJ/pulse) was also measured to be around 60%.

Figure 3d is a CID mass spectrum obtained by introducing argon as a collision gas in the ion trap. Since the CID experiment was done without mass selection, some of the fragment ions in the mass spectrum may not be from dissociation of YAH^+. By comparing the CID spectrum with that obtained by a triple quadrupole mass spectrometer (API 3000), we

Table 1. Fragment ions of YAH$^+$ and GWH$^-$ by PID and CID

YAH$^-$			GWH$^-$		
Fragments	CID	PID	Fragments	CID	PID
236	NH$_3$ loss		244	MH$^+$-18	
136	a$_1$	a$_1$	216	(H$_2$O+CO) loss	
			188	z$_1$	z$_1$
			170	z$_1$-H$_2$O	
			159	W immonium ion^a	
			146		z$_1$-CH$_2$CO
			132		4-amino indole ion^b
			130		W side chain ion^a

^{a}ref. 28, ^{b}ref. 9.

found that the fragments of m/z 136 and 236 are from CID of YAH$^+$. It is not certain yet, however, about the origins of the other fragment ions in Figure 3d. The fragment ions detected in the PID and the CID mass spectrum of YAH$^-$ are listed in Table 1.

Figure 4a is the mass spectrum of GWH$^-$. The singly charged GWH$^-$ is also the strongest peak in the mass spectrum. Figure 4b is the difference spectrum of the laser-on minus the laser-off signals at 277 nm. Figure 4c is the CID spectrum obtained using argon as a collision gas. The observed fragments are summarized in Table 1.

The main fragment ions in the PID spectrum are m/z 130 and 188, which is somewhat consistent with the result of protonated leucine-tryptophan ions (LWH$^+$).[22] These fragment ions including those of m/z 132 and 146 were also observed in the previous PID of WH$^-$,[9] which indicates that these ions are from dissociation of the tryptophan residue of GWH$^-$. The fragment ions of m/z 216 and 244 that have strong intensity in the CID spectrum are absent in the PID spectrum. This clearly shows that the dissociation mechanisms between the PID and the CID of GWH$^-$ are indeed quite different.

It is well known that PID is more sequence- and site-specific than CID, due to the non-statistical nature of dissociation occurring at the specific excited states accessible by one or multiphoton absorption. Correspondingly, for PID with UV beams, it was insisted that the presence of an aromatic chromophore such as a tryptophanyl, a tyrosyl and a phenylalanyl residue in the protonated peptide ions enhances dissociation in its vicinity while the absence of the chromophore results in nonspecific, statistical dissociation.[23] This is called as the chromophore effect of PID.[24,25]

In the PID spectrum of GWH$^+$, we insist that the fragment ion of m/z 188 is from non-statistical dissociation, exhibiting the chromophore effect of the tryptophanyl residue, with following reasons: First, it was reported that the fragment of m/z 188 is produced by selective C$_\alpha$-N bond rupture of WH$^+$ or LWH$^+$ in the higher excited state.[22,26] Second, the fragment of m/z 188 is produced by dissociation of the bond in the vicinity of the tryptophanyl residue. Third, the fragment
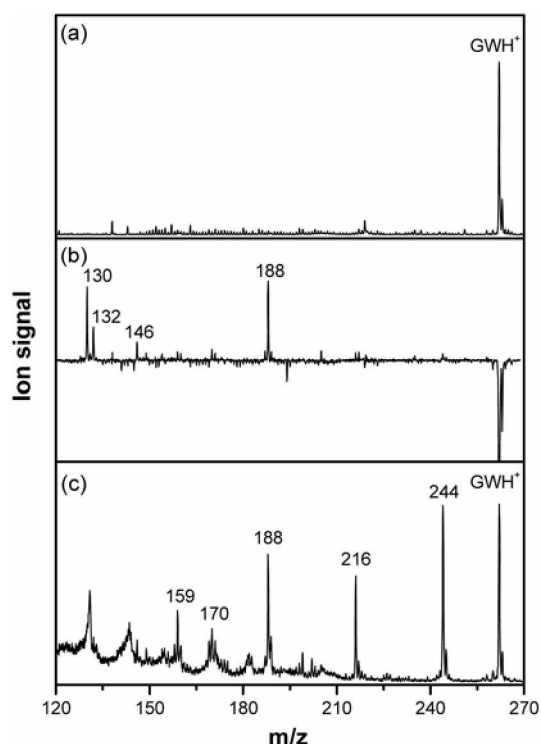

Figure 4. (a) Mass spectrum of GWH$^+$ with helium in the ion trap. (b) Difference spectrum obtained by subtracting the laser-off signals from the laser-on. The laser-on signals were obtained by irradiating laser pulses (2 mJ/pulse) at 277 nm onto the ions in the QIT. (c) CID spectrum obtained by introducing argon into the QIT as a collision gas.

of m/z 188 is detected as one of the main fragments in the PID spectrum.

The fragment ion of m/z 188 is also found in the CID of GWH$^+$. However, different from the case of PID, the fragment ion in the CID is more likely to be from statistical dissociation occurring at the electronic ground state.

Interestingly, the fragment ion of m/z 217 from dissociation of the other end of the tryptophanyl residue (*i.e.* the C$_\alpha$-C bond) is absent in the PID spectrum. This was also true in the PID of LWH$^+$.[22] On the contrary, however, if the tryptophanyl residue was at the N-terminus like the protonated Trp-Ala ion (WAH$^-$), the fragment ion of m/z 159 from the C$_\alpha$-C dissociation of the tryptophanyl residue became dominant while that of m/z 259 from the C$_\alpha$-N dissociation was very small.[27] This indicates that the dissociation of the bond close to a C- or an N-terminus of peptide ions may require much higher energy than that of the same bond located far from both termini, although the bond is in the vicinity of the tryptophanyl residue. It is worth noting that the fragment ions from dissociation of either ends of a tryptophanyl residue had similar intensities in the PID of GWGH$^+$,[28] where both ends of the residue are far from the C- and N-terminus.

In summary, QIT-TOFMS has been constructed in our laboratory and successfully used to study PID of protonated dipeptide ions produced by ESI. The CID spectra of YAH$^+$ and GWH$^+$ were also obtained in the QIT-TOFMS and com-

pared to their respective PID spectra. In the PID of GWH⁻, the fragment ion of m/z 188 was suggested to be from non-statistical dissociation, exhibiting the chromophore effect of PID. Analyzing the PID spectra of several protonated di- and tri-peptide ions with a tryptophanyl residue, we found that the chromophore effect plays an important role in the PID of the peptide ions. The studies of measuring the wavelength dependence of PID are on the way to understand the dissociation mechanisms of protonated peptide ions that give rise to the chromophore effect.

References

1. Douglas, D. J.; Frank, A. J.; Mao, D. *Mass Spectrom. Rev.* **2005**, *24*, 1.
2. Gabryelski, W.; Li, L. *Rapid Commun. Mass Spectrom.* **2002**, *16*, 1805.
3. Weickhardt, C.; Moritz, F.; Grotemeyer, J. *Mass Spectrom. Rev.* **1996**, *15*, 139.
4. Paul, W. *Angew. Chem. Int. Ed. Engl.* **1990**, *29*, 739.
5. Parks, J. H.; Pollack, S.; Hill, W. *J. Chem. Phys.* **1994**, *101*, 6666.
6. Peng, W.-P.; Yang, Y.-C.; Kang, M.-W.; Lee, Y. T.; Chang, H.-C. *J. Am. Chem. Soc.* **2004**, *126*, 11766.
7. Michael, S. M.; Chien, M.; Lubman, D. M. *Rev. Sci. Instrum.* **1992**, *63*, 4277.
8. Oomens, J.; van Roij, A. J. A.; Meijer, G.; von Helden, G. *Astrophys. J.* **2000**, *542*, 404.
9. Kang, H.; Dedonder-Lardeux, C.; Jouvet, C.; Martrenchard, S.; Gregoire, G.; Desfrancois, C.; Schermann, J.-P.; Barat, M.; Fayeton, J. A. *Phys. Chem. Chem. Phys.* **2004**, *6*, 2628.
10. Thompson, C. J.; Husband, J.; Aguirre, F.; Metz, R. B. *J. Phys. Chem. A* **2000**, *104*, 8155.
11. Metz, R. B. *Int. J. Mass Spectrom.* **2004**, *235*, 131.
12. Hu, Y.; Hadas, B.; Davidovitz, M.; Balta, B.; Lifshitz, C. *J. Phys. Chem. A* **2003**, *107*, 6507.
13. Gregoire, G.; Kang, H.; Dedonder-Lardeux, C.; Jouvet, C.; Desfrancois, C.; Onidas, D.; Lepere, V.; Fayeton, J. A. *Phys. Chem. Chem. Phys.* **2006**, *8*, 122.
14. Purves, R. W.; Gabryelski, W.; Li, L. *Rapid Commun. Mass Spectrom.* **1998**, *12*, 695.
15. Chen, Y.; Jin, X.; Misek, D.; Hinderer, R.; Hanash, S. M.; Lubman, D. M. *Rapid Commun. Mass Spectrom.* **1999**, *13*, 1907.
16. Wang, L.-S.; Ding, C.-F.; Wang, X.-B.; Barlow, S. E. *Rev. Sci. Instrum.* **1999**, *70*, 1957.
17. He, L.; Liu, Y.-H.; Zhu, Y.; Lubman, D. M. *Rapid Commun. Mass Spectrom.* **1997**, *11*, 1440.
18. Hashimoto, Y.; Waki, I.; Yoshinari, K.; Shishika, T.; Terui, Y. *Rapid Commun. Mass Spectrom.* **2005**, *19*, 221.
19. Campbell, J. M.; Collings, B. A.; Douglas, D. J. *Rapid Commun. Mass Spectrom.* **1998**, *12*, 1463.
20. Purves, R. W.; Gabryelski, W.; Li, L. *Rev. Sci. Instrum.* **1997**, *68*, 3252.
21. Boyarkin, O. V.; Mercier, S. R.; Kamariotis, A.; Rizzo, T. R. *J. Am. Chem. Soc.* **2006**, *128*, 2816.
22. Nolting, D.; Schultz, T.; Hertel, I. V.; Weinkauf, R. *Phys. Chem. Chem. Phys.* **2006**, *8*, 5247.
23. Oh, J. Y.; Moon, J. H.; Kim, M. S. *J. Mass. Spectrom.* **2005**, *40*, 899.
24. Moon, J. H.; Yoon, S. H.; Kim, M. S. *Bull. Korean Chem. Soc.* **2005**, *26*, 763.
25. Oh, H. B.; McLafferty, F. W. *Bull. Korean Chem. Soc.* **2006**, *27*, 389.
26. Kang, H.; Dedonder-Lardeux, C.; Jouvet, C.; Gregoire, G.; Desfrancois, C.; Schermann, J.-P.; Barat, M.; Fayeton, J. A. *J. Phys. Chem. A* **2005**, *109*, 2417.
27. Gabryelski, W.; Li, L. *Rev. Sci. Instrum.* **1999**, *70*, 4192.
28. Gregoire, G.; Dedonder-Lardeux, C.; Jouvet, C.; Desfrancois, C.; Fayeton, J. A. *Phys. Chem. Chem. Phys.* **2007**, *9*, 78.